Genetic Remodeling and Transcriptional Remodeling of Subtelomeric Heterochromatin Are Different†

Sabrina Venditti,*,‡ Glauco Di Stefano,‡ Manuela D'Eletto,‡ and Ernesto Di Mauro‡,§,||

Centro di Studio per gli Acidi Nucleici (CNR), Fondazione Istituto Pasteur, Fondazione Cenci Bolognetti, and Dipartimento di Genetica e Biologia Molecolare, Universita' di Roma La Sapienza, P. le A. Moro 5, 00185, Roma, Italy

Received December 14, 2001; Revised Manuscript Received February 14, 2002

ABSTRACT: The structure, the extension, and the regulatory functions of telomeric and subtelomeric heterochromatin are not completely understood partly due to the difficulty of separating structural from functional features. We have previously observed that genetic alterations of telomeric heterochromatin components relieve transcriptional silencing. We have developed an analytical system allowing the separate determination of the effects of transcription and of genetic alterations on the subtelomeric structures. The uncoupled analysis, performed on the left extremity of chromosome III of *Saccharomyces cerevisiae*, consists of genetic dissections, induction of transcription of a resident gene, and chromatin analysis. The results allow (i) the determination of the precise localization and of the extension of heterochromatin (here from 0.9 to 2.6 kb from the innermost extremity of the $C_{1-3}A$ tract) and (ii) the definition of the transcription and of the genetically induced chromatin remodelings and of their marked differences, thus allowing (iii) specific analyses of the structural effects of the genetic modification of the heterochromatin components.

Although not cytologically detectable as in higher eukaryotes, *Saccharomyces cerevisiae* telomeric chromatin shows the functional characteristics of heterochromatin, such as late replication, resistance to nucleases, and position effects on the genes located in their vicinity (*1*). Coupled with the repetitive nature of telomeric and subtelomeric DNA sequences (both locally and among different chromosomal ends), these two latter properties make the analysis of telomeric chromatin structure and of its function particularly difficult. The scarcity of data on the transcription of naturally occurring genes in subtelomeric regions adds to this difficulty.

Telomeric position effect (TPE)[1] is exerted through the involvement of the silent information regulators, Sir3p, Sir2p, and Sir4p. Deletion of each Sir protein causes loss of telomeric transcriptional silencing (*2*).

From the structural point of view a number of studies have revealed that telomeres are covered with a complex aggregate of Sir proteins that in yeast is responsible for all of the properties mentioned above. This aggregate includes several components such as the SIR proteins, along with Rif1p and Rif2p (*3*, *4*), and the Ku proteins involved in DNA repair and recombination (*5*, *6*).

The Sir complex starts its nucleation from the terminal telomeric repeats, due to the ability of the Sir proteins to bind Rap1p, which in turn directly binds DNA at sites encompassed in the sequence-repetitive region (*7*, *8*). The Sir proteins spread along the subtelomeric regions interacting with each other and with the N-terminal tails of histones H3 and H4 (*9*). The diffusion by spreading is reinforced by the folding back of the chromosome end onto the subtelomeric region, according to a model based on chromatin immunoprecipitation analysis (*7*). Lack of any one of the Sir proteins causes disruption of the complex, indicating that its integrity is required for the correct organization of the heterochromatin structure (*7*). The individual functions of the Sir proteins have been clarified only partially, making it difficult to define how they affect telomeric heterochromatin from a biochemical point of view. However, some evidence points to the involvement of the Sir proteins in the organization of the underlying repressive nucleosome structure.

First, Sir2p, which participates in the complex through interaction with Sir4p, was recently described to have NAD-dependent histone deacetylase activity (*10*, *11*). Substrates for this activity were shown to be Lys9 and Lys14 of histone H3 and Lys16 of histone H4, located in the histone domains involved in the interaction with Sir3p and Sir4p (*9*, *12*).

A second line of evidence comes from previous work on a *S. cerevisiae* Ty5-1 element present in subtelomeric position on the left arm of chromosome III. Being defective for transposition, this element is unique in the yeast genome.

† This work was supported by CNR Target Project on Biotechnology, by MURST 5% project Biomolecole per la Salute Umana, and by MURST 40% Projects.

* To whom correspondence should be addressed. E-mail: sabrina.venditti@uniroma1.it. Phone: +11.39.06.49912659. Fax: +11.39.06.49912500.

‡ Dipartimento di Genetica e Biologia Molecolare.

§ Centro di Studio per gli Acidi Nucleici (CNR).

|| Fondazione Istituto Pasteur, Fondazione Cenci Bolognetti.

[1] Abbreviations: SIR, silent information regulator; TPE, telomeric position effect; MNase, micrococcal nuclease; LTR, long terminal repeat; PRE, pheromone response element.

10.1021/bi016052y CCC: $22.00
Published on Web 03/20/2002

Ty5-1 undergoes telomeric position effect (*13*), meaning that it is normally silent in wild-type strains and can be transcribed in strains mutant for or lacking heterochromatin components such as Sir3p or the N-terminal tail of histone H4. The nucleosome positioning of this subtelomeric region is also directly affected by the presence/absence of Sir3p and by modifications of histone H4. Both types of mutations in fact cause a similar change in the nucleosomal organization (*14*), indicating that establishment of in vivo repressive structure requires recruitment of Sir3p through interaction with the N-terminal tail of H4 (*15*).

Other evidence for a heterochromatin component directly contacting the nucleosome was documented recently in *Drosophila* heterochromatin. The direct binding of HP1 (heterochromatin protein 1) to nucleosomes (*16*) was reported. The binding involves the HP1 chromodomain and is mediated by methylation of histone H3 at Lys9 (*17*, *18*). This evidence suggests that HP1 may function as a bridge between nucleosomes and non-histone protein complexes to form higher order chromatin structure.

Retrotransposons belonging to the Ty5 family have been described to preferentially transpose in heterochromatic regions of the *S. cerevisiae* genome (*19*). In this way Ty5 elements reach a compromise with the cell reducing their own level of transcription, hence limiting the mutagenic potential of transposition (*20*). Members of the Ty5 family inserted at several heterochromatin locations were described to be silenced and subjected to transcriptional induction by the pheromone response pathway (*21*). In fact, the LTRs of these elements contain PREs (pheromone response elements) which respond to mating factors. No evidence has yet been reported for the induction of transcription of the telomerically located Ty5-1.

Telomeric silencing can be overcome by a transactivator in a system in which the *URA3* gene was relocated at yeast telomere VII-L (*22*), indicating that repressive chromatin is not completely refractory to transcription complex access. This was confirmed by a study that showed TBP and Pol II access to repressive *SIR*-generated heterochromatin, following the binding of the Hsfp activator to a yeast heat shock gene, flanked by *HM* silencers (*23*).

Despite all the observations describing the relieving of telomeric silencing, the dynamics of possible chromatin and heterochromatin modifications related to transcription at telomeres have not been investigated in detail. An exception is the recent report showing that transcription induced through the telomeric $(C_{1-3}A)_n$ repeats disrupts core heterochromatin by eliminating Rap1p-mediated telomere looping (*24*).

In this work we have asked whether transcription of the Ty5-1 element located at chromosome LIII could be induced by α-factor and, if so, whether there was an influence on chromatin structure in the subtelomeric region. We have also analyzed the transcription and the chromatin structure in several mutants, in particular in strains bearing mutations of H3 and H4 N-terminal domains or carrying deletions of *SIR* genes. We investigated whether these mutants showed alternative nucleosomal organizations (as previously reported for the *sir3* mutant strain; *14*) in order to understand if the overall integrity of the silencing complex has an influence on the underlying nucleosomal arrangement. Finally, we have analyzed to what extent the chromatin structure of Ty5-1 in the mutants can be distinguished from that of α-factor-induced cells, to define the chromatin characteristics specific for each condition.

MATERIALS AND METHODS

Yeast Strains and Growth Conditions. All strains used were provided by M. Grunstein.

(A) Histone Mutants: PKY501, *MAT***a** *ade2-101 his3-*Δ*200 leu2-3 leu2-112 lys2-801 trp1-*Δ*901 ura3-52 thr tyr arg4-1 hhf1::HIS3 hhf2::LEU2*/pPK301 (*CEN3 URA3 ARS1 HHF2*); PKY813, isogenic to PKY501 containing pPK613 (*CEN3 URA3 ARS1 hhf2*Δ*4*−*28*); LJY912, isogenic to PKY501 containing pLJ912 (*CEN3 URA3 ARS1 hhf2-K16Q*); LJY933, isogenic to PKY501 containing pLJ933 (*CEN3 URA3 ARS1 hhf2-H18G*); LJYD24P, isogenic to PKY501 containing pLJD24P (*CEN3 URA3 ARS1 hhf2-D24P*); RMY420, *MAT***a** *ade2-101 his3-*Δ*200 leu2-2,112 trp1-*Δ*901 ura3-52 lys2-801 hht1, hhf1::LEU2 hht2, hhf2::HIS3/* pRM420 (*CEN4 ARS1 TRP1 HHF2 hht2*Δ*4*−*20*); RMY430, same as RMY420 containing pRM430 (*CEN4 ARS1 TRP1 HHF2 hht2*Δ*4*−*30*).

(B) SIR Mutants: LJY155, *MAT***a** *ade2-101 his3-*Δ*200 leu2-3,112 lys2-801 trp1-*Δ*901 ura3-52 hhf1::HIS3 sir3::LEU2/*pRS424 (2*μ* TRP1); STY30, *MAT***a** *ade2-101 his3-*Δ*200 leu2-3,112 lys2-801 trp1-*Δ*901 ura3-52 thr tyr adh4::URATELVII-L sir3::SIR3HA/HIS3 sir2::TRP1*; STY36, same as STY30 *sir4::TRP1*.

Mutant strains in histone H4 were grown at 28 °C in Synthetic Complete (SC) medium lacking uracil and containing glucose to an A_{600} of about 0.3−0.4/mL. Mutant strains in histone H3 and SIR proteins were grown similarly in SC medium lacking tryptophan.

α-Factor Treatment. α-Factor treatment for both transcriptional and chromatin analysis was carried out as follows: cultures were grown in the appropriate medium to the log phase. An aliquot of cells was collected for RNA or chromatin analysis to serve as control, while the rest of the culture was divided into aliquots and treated with increasing amounts of α-factor (see legends to the figures) for 80 min. Following treatment cells were collected by centrifugation and analyzed.

Micrococcal Sensitivity Analysis. Cells from 50 mL cultures were grown to the exponential phase, collected by centrifugation, and treated with zymolyase (Seikagaku) to remove the cell wall. Spheroplasts were permeabilized with nystatin (Sigma) (*25*) to allow introduction of increasing amounts of micrococcal nuclease (MNase, purchased from Roche). The MNase amounts used are specified in the legends to the figures. After digestion of chromatin (in vivo) or deproteinized genomic DNA (in vitro) the sensitivity to MNase was analyzed by the indirect end-labeling technique (*26*). DNA samples were purified, digested with *Bam*HI (Roche), resolved on agarose gels, and transferred to nylon membranes. The nuclease cleavage profile was visualized after hybridization with the probes indicated in the legend to the figures, adjacent to the *Bam*HI site on both sides. The probes were produced by PCR amplification using the oligonucleotides described below.

Transcription Analysis by RT-PCR. RNA was extracted by the hot phenol protocol from all strains and purified (*27*). DNase I treatment to remove residual DNA was performed

for 30 min at 37 °C, using 40 units of DNase I (Roche). Reverse transcription was carried out with equal amounts of RNA using MMLV reverse transcriptase (Superscript II, Gibco BRL), and oligo(dT)$_{12-18}$ for first-strand cDNA synthesis.

PCR amplifications of the reverse transcription products were performed using 2.5 units of AmpliTaq (Perkin-Elmer) in the presence of the specific oligonucleotides described below.

Oligonucleotides. The oligonucleotides used in the amplification step of the RT-PCR assays for Ty5-1 were the same as the ones used to produce probe 1 in the chromatin analysis and are the following: oli1, 5′ TGT ACG GTA TCG AGA CCG CTG CTG AAT 3′ (map position: 1495−1522); oli1c, 5′ CAG CGA CCC TTC CAA GCG AAT CAT CAC 3′ (map position: 1699−1725). The oligonucleotides used to produce probe 2 are the following: oli2,: 5′ CCA GGC TTA CTC TTA TAG AGG 3′ (map positions: 1771−1791); oli2c, 5′ GAG TCA CCG AAT TTC TCG TGG 3′ (map positions: 1968−1988). The oligonucleotides used for the transcription analysis of *FUS1* are the following: fus5′, 5′ GCA ATG TCT ACT ACC TTA GCA 3′; fus3′, 5′ GAT GGG AAG TCC GAT TGA AAG 3′. For the amplification of *ACT1* the following oligos were used: act5′, 5′ GTTGCTGCTTTGGTTATTGA 3′; act3′, 5′ AGCTTCATCACCAACGTAGG 3′.

RESULTS

Induction of Ty5-1 Transcription by α*-Factor*. Ty elements are normally repressed by heterochromatin but can be induced by a number of stimuli, among which are treatment with α-factor in cells of mating type **a** due to the presence of PREs (pheromone response elements) in the LTR regions. Transcription of Ty5s inserted in various heterochromatin locations was shown to occur following treatment with α-factor (*21*). However, evidence for the induction of transcription of the Ty5-1 located in the chromosome III left telomere by α-factor is not reported. We found that this element can be transcribed in strains bearing heterochromatin mutations (*13*), such as deletion of *SIR3* and of the histone H4 N-terminal tail, and that these mutations are correlated with an alternate nucleosome organization. We therefore asked whether this element could be induced by α-factor to transcribe in wild-type strains and, if so, which is the nucleosomal organization in the regulatory region under transcribing conditions.

Cultures of wild-type cells were grown to the cell density of 0.3 OD$_{600}$/mL and then treated with increasing amounts of α-factor to detect Ty5-1 transcription (Figure 1B). Cells were harvested after 80 min of exposure to the pheromone, and RNA was extracted. Following DNase I treatment the purified RNA was subjected to RT-PCR reactions, using a couple of oligonucleotides which amplify a 230 bp fragment in the first ORF of the Ty5-1. The positions of the oligonucleotides are indicated in the linear map of this region in Figure 1A. The 230 bp band is observed after treatment with 1 μM α-factor (Figure 1B, lane 2), while it is absent in the untreated wild-type, in agreement with previously reported results (*13*). Increasing the amount of α-factor to 3.5 μM (Figure 1B, lane 3) and up to 10 μM (data not shown) does not cause further increase of mRNA levels. As a control,

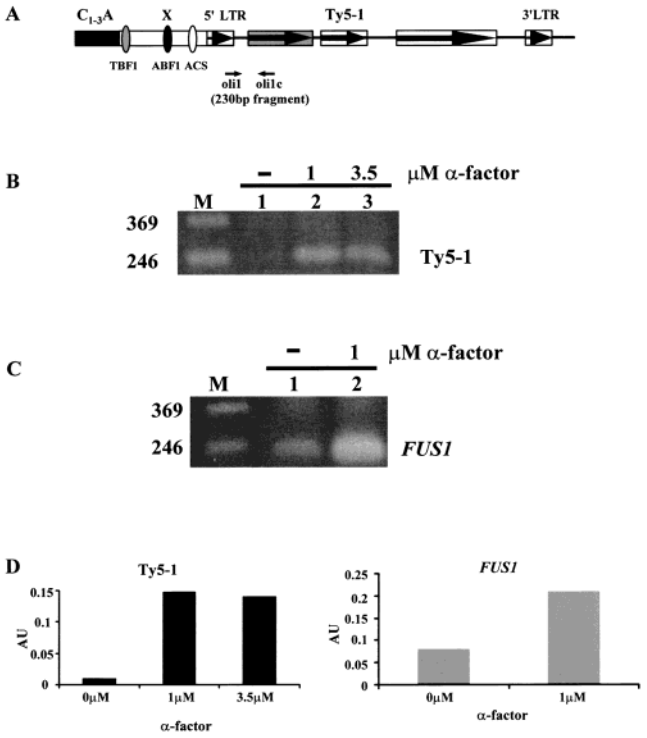

FIGURE 1: Induction of Ty5-1 transcription by α-factor. (A) Schematic map of chromosome LIII telomeric region. All of the elements present in this region are indicated: $C_{1-3}A$ telomeric repeats, subtelomeric X element, and Ty5-1 retrotransposon delimited by 5′ and 3′ LTRs. Sites for binding of TBF1, ABF1, and ACS are indicated. (B) RT-PCR analysis of Ty5-1 expression in wild-type cells (strain PKY501) following α-factor treatment for 80 min at 30 °C. Cells were either untreated (lane 1) or treated with 1 μM (lane 2) or 3.5 μM (lane 3) α-factor. PCR amplification of a 230 bp fragment in the Ty5-1 first ORF was achieved using oligonucleotides oli1 and oli1c [depicted in (A) and described in Materials and Methods]. (C) RT-PCR assay of the *FUS1* gene as a control for α-factor effectiveness. *FUS1* is expressed at the basal level in untreated cells (lane 1) and is induced after treatment with 1 μM α-factor (lane 2). The oligos used for PCR amplification are described in Materials and Methods. M = 123 bp molecular weight marker. (D) Quantitative analysis of PCR products for Ty5-1 and *FUS1*. AU = arbitrary units.

the same RNA extracted from α-factor-treated cells was used in RT-PCR reactions using a couple of oligos which amplify the coding region of the *FUS1* gene (Figure 1C). *FUS1* is normally expressed at a basal level in untreated cells (Figure 1C, lane 1) and was described to be induced by pheromones (Figure 1C, lane 2; *28*). Figure 1D shows a quantification of the PCR products for both Ty5-1 and *FUS1*.

These results show that the Ty5-1 naturally present in subtelomeric location at chromosome III can be induced to transcribe by conditions other than the loss of heterochromatin proteins or histone mutations.

Chromatin Structure of the LIII Subtelomeric Region in Pheromone-Treated Cells. As mentioned above, derepression of Ty5-1 transcription in strains lacking *SIR3* or the 4−28 N-terminal portion of histone H4 [H4Δ(4−28)] is accompanied by a nucleosomal configuration in the LTR, whose chromatin structure is quite different from that of the chromatin observed in wild-type strains. Three nucleosomes covering this region are present in completely alternate positions in *sir3* and H4Δ(4−28) as compared to wild-type (*14*, *15*). This situation is schematically illustrated on the

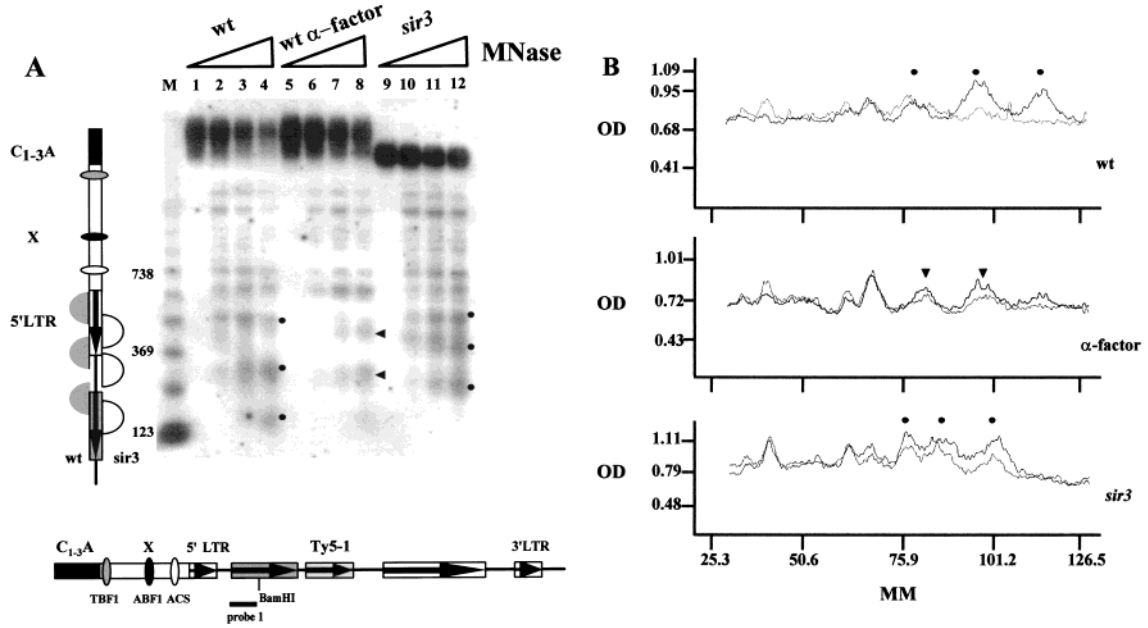

FIGURE 2: (A) Chromatin structure of the subtelomeric LIII region in α-factor-treated cells. Comparison, by indirect end labeling, between MNase cleavages of wild-type cells (lanes 1−4) and wild-type cells treated with 1 μM α-factor (lanes 5−8) to define nucleosome positioning in the subtelomeric region. The profiles are also compared to that of *sir3* cells (strain LJY155, lanes 9−12). Triangles represent increasing amounts of MNase: 0, 1.25, 2.5, and 5 units/mL for each strain. The schematic map reported on the left side of the figure indicates the positions of the nucleosomes located in the LTR sequence for the wild type and the *sir3* strain. The positions are based on the alternate patterns indicated by black dots. Sites of hyperaccessibility to MNase over the LTR region in α-factor-treated cells are indicated by arrowheads. The position of probe 1, abutting the *Bam*HI site, used for the indirect end labeling, is indicated in the map underneath the panel. M = 123 bp molecular weight marker. (B) Densitometric analysis of two samples for each condition shown in panel A. Lighter tracings: lanes 2 (wt), 6 (α-factor), and 10 (*sir3*). Darker tracings: lanes 4 (wt), 8 (α-factor), and 12 (*sir3*). Dots and arrowheads as in panel A.

left side of Figure 2A, where nucleosomes are indicated as gray semicircles for the wild type and as empty semicircles for the *sir3* strains. Their positioning is based on the alternate profiles indicated by black dots in the figure.

The observed induction of transcription of Ty5-1 by α-factor allows us to ask whether the nucleosomes in transcribing subtelomeres adopt the same alternate organization.

We performed the chromatin analysis using micrococcal nuclease (MNase) in vivo on pheromone-treated cells. After 80 min of exposure to the pheromone, a fraction of cells from the same culture used for the transcriptional analysis was collected and treated with increasing amounts of MNase, following permeabilization of spheroplasts by nystatin. Figure 2A compares the chromatin structure of the LIII subtelomeric region of α-factor-treated wild-type cells (lanes 5−8) with the *sir3* strain (lanes 9−12), analyzed by the indirect end-labeling technique using probe 1. The results clearly show for the pheromone-treated cells an increase of MNase accessibility (lanes 5−8) localized in the Ty5-1 LTR, indicated by the arrowheads. Globally, the nucleosome profile in the transcribed wild-type resembles more that of the wild-type nontranscribing cells (lanes 1−4) than that of the *sir3* transcribing (*14*) strain. In the transcribing wild-type, though, the bands representing the borders of the nucleosomes on the LTR are less defined and more accessible to MNase than in the nontranscribing condition. Hyperaccessibility is observed already at the lower concentrations of enzyme (compare lane 6 with lane 2), indicating that most of the population is involved in this alteration. A densitometric analysis of this experiment is shown in Figure 2B. Two samples for each condition were chosen, namely, lanes 2 and 4 for the wt, lanes 6 and 8 for the α-factor-treated wt, and lanes 10 and 12 for the *sir3* strain. The peaks of interest are indicated using the same dot and arrowhead code as in panel A.

It is interesting that the profile of α-factor-treated cells is indeed different from that observed for the *sir3* strain: induction of transcription by α-factor does not lead to a conformational change as extended as does the lack of Sir3p. Comparison of α-factor-induced profiles (lanes 5−8) with the wild-type control (lanes 1−4) suggests that the structure of the LTR region after induction by α-factor is not drastically rearranged and is characterized by a less tight positioning of the nucleosomes, whose borders become more accessible to MNase.

This result also implies that the previously described structure of the Ty5-1 chromatin in the *sir3* strain (*14*) is not merely a consequence of transcriptional derepression, but it is strictly linked to the presence of heterochromatin components such as Sir3p, suggesting that disruption of heterochromatin higher order structure has profound effects on the underlying nucleosomal distribution.

Nucleosomal Organization in Strains Carrying Heterochromatin Mutations. (A) Sir Mutations. Sir3p is involved in the heterochromatin organization at telomeres in combination with Sir2p and Sir4p. SIR proteins form a complex through interactions with specific portions of the N-terminal tails of histones H3 and H4. Having described (*14*, *15*) the transcriptional and structural consequences of deleting either *SIR3* or the N-terminal tail of histone H4, we decided to investigate in more detail the relationship between other heterochromatin elements and the nucleosomal organization of Ty5-1. At this purpose the MNase cleavage profiles of

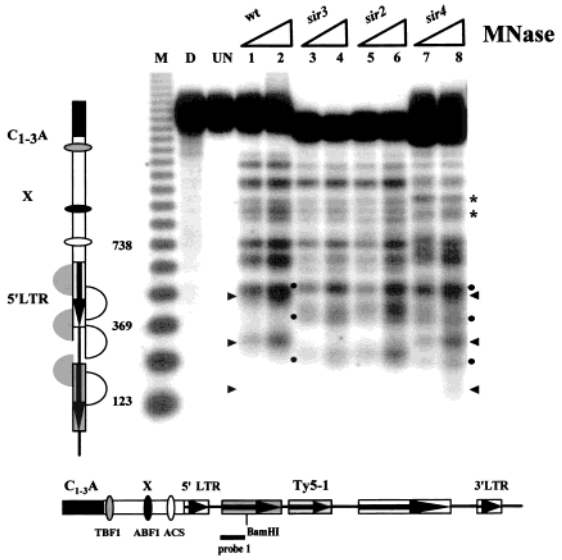

FIGURE 3: Nucleosomal organization of the subtelomeric LIII region in strains bearing mutations in the *SIR* genes. Nucleosomal analysis by indirect end labeling of in vivo MNase accessibility sites in wild-type (strain PKY501, lanes 1 and 2), *sir3* (strain LJY155, lanes 3 and 4), *sir2* (strain STY30, lanes 5 and 6), and *sir4* (strain STY36, lanes 7 and 8). For each strain 1.25 and 5 units/mL MNase were used in the in vivo assay. UN = untreated DNA. D = control; genomic DNA was purified and treated in vitro with 1.25 units/mL MNase. MNase accessibility sites typical of the wild-type profile are indicated by arrowheads. M = molecular weight marker. Alternative bands related to the *sir3* mutant profile are indicated by black dots. The intermediate characteristics of the *sir4* profile (showing both types of bands) are marked on the right side of the panel. Additional differences in the *sir4* strain, as compared to both wild-type and *sir3*, are located inside the X element indicated by asterisks. The schematic vertical map on the left summarizes the nucleosomal organization of wild-type (gray semicircles) and *sir3* (empty semicircles). The map underneath the panel indicates the location of probe 1 and of the *Bam*HI site.

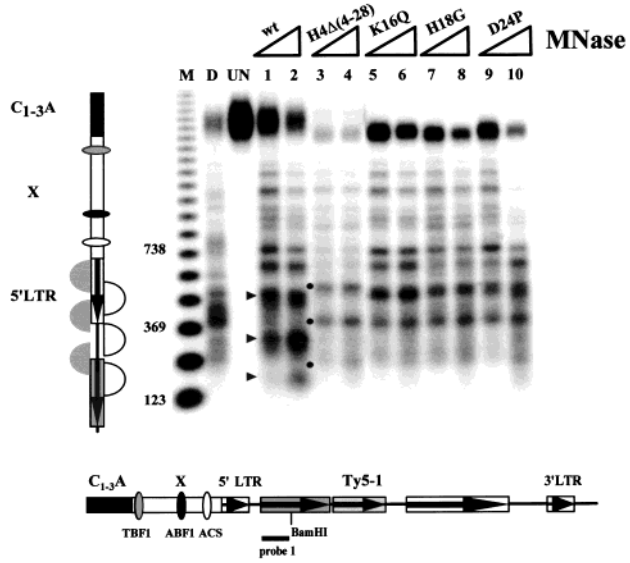

FIGURE 4: Change of nucleosome distribution in the LTR of Ty5-1 of several strains carrying mutations in the N-terminus of H4. Chromatin analysis by indirect end labeling of the following mutant strains: K16Q (Lys16Glu, strain LJY912, lanes 5 and 6), H18G (His18Gly, strain LJY933, lanes 7 and 8), and D24P (Asp24Pro, strain LJYD24P, lanes 9 and 10). MNase profiles are compared to those of wild-type (strain PKY501, lanes 1 and 2) and H4Δ(4−28) (strain PKY813, lanes 3 and 4). The amounts of MNase used for each strain are 1.25 and 5 units/mL. The profiles of the three strains carrying point mutations are identical to that of the (4−28) deletion strain. The bands typical of the mutant pattern (black dots) in the LTR of Ty5-1 are alternate to those of the wild type (arrowheads). UN = untreated DNA. D = genomic DNA treated in vitro with 1.25 units/mL MNase. M = molecular weight marker. The schematic vertical map on the left summarizes the nucleosomal organization of wild-type (gray semicircles) and *sir3* (empty semicircles). The map underneath the panel indicates the location of probe 1 and of the *Bam*HI site.

several mutant strains, among which *sir2* and *sir4* and strains bearing either point mutations in the N-terminal tail of H4 or N-terminal deletions of H3, were analyzed. All of the profiles were compared with those of the wild type and the *sir3*, taken as reference for the *sir* mutant strains, or of the H4Δ(4−28), taken as reference for the histone mutants.

First we analyzed the nucleosome profile of *sir2* and *sir4* strains. The results of the in vivo MNase digestion are shown in Figure 3. The *sir2* strain (lanes 5 and 6) shows the same MNase cleavage pattern of *sir3* (lanes 3 and 4) over the entire subtelomeric region. In addition, the bands typical of the LTR profile, indicated by the black dots, are also present in *sir2* at the same positions. This result indicates that Sir2p, like Sir3p, may play a role in the positioning of nucleosomes in heterochromatin. As for *sir4*, it appears that its chromatin organization in the LTR region is intermediate between that of wild type and that of *sir3*. In fact, its MNase profile shows (lanes 7 and 8) the presence of bands resembling both wild-type (arrowheads) and *sir3* (black dots) chromatins, suggesting that Sir4p is only partially involved in the nucleosome organization of this region. In addition, in *sir4* also a tract of the subtelomeric X element shows a different pattern of bands, indicated by the asterisks (right side of Figure 3). It is therefore possible that the function of Sir4p is only indirectly linked to the nucleosome organization and that it correlates with other functions of the subtelomeric X element.

(B) Histone Mutations. Our earlier results highlighted that deletion of residues 4−28 of H4 mimics the chromatin rearrangements caused by loss of Sir3p (*15*). This domain of H4 contains residues required for the Sir3p−H4 in vivo and in vitro interaction (*9*, *29*). Therefore, we analyzed by in vivo MNase several strains bearing point mutations in the N-terminal tail of H4. In detail, we have chosen substitutions at residues Lys16, His18, and Asp24 which are changed to Glu, Gly, and Pro, respectively. All three residues were shown to be required for transcriptional silencing in vivo (*29*) and their mutation to affect the Sir3p−H4 interaction in vitro (*9*). Figure 4 shows the nucleosomal distribution in the LTR region of Ty5-1 for each of the three substitution mutants analyzed, in comparison with the wild-type and the H4Δ(4−28) profiles. It is evident that all of the mutations in the Sir3p−H4 interaction domain affect the nucleosomal organization identically, since the pattern of bands in the LTR is the same as in H4Δ(4−28) for all of the strains. This result supports the relevance of the Sir3p−H4 interaction in the heterochromatin organization and, ultimately, the involvement of the Sir complex in the translational positioning of nucleosomes.

Histones H4 and H3 are both involved in the maintenance of the integrity of heterochromatin structures. Deletions in the N-terminal tail of H3 cause loss of silencing both at telomeres and at *HM* loci, although the level of transcription

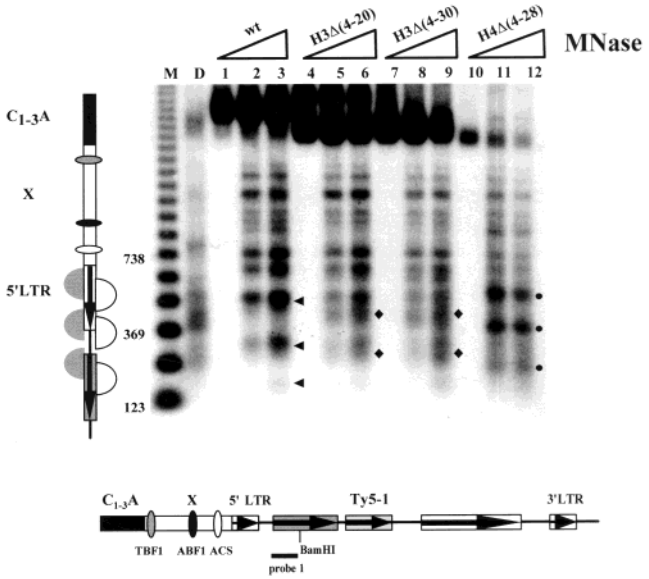

FIGURE 5: Effects of H3 N-terminal deletions on the chromatin structure of the LTR of Ty5-1. Strains H3Δ(4−20) (RMY420, lanes 4−6) and H3Δ(4−30) (RMY430, lanes 7−9) were subjected to in vivo MNase analysis to compare the profiles in the LTR of the Ty5-1 with those of the wild type (PKY501, lanes 1−3) and H4Δ-(4−28) (PKY813, lanes 10−12). Lanes 1, 4, 7, and 10: no MNase. For each strain the amounts of MNase used are 1.25 and 5 units/mL. The H3 mutants show profiles of accessibility to MNase different from both wild type and H4Δ(4−28). The sites of hyperaccesibility are indicated by black diamonds, while the wild-type profile is indicated by arrowheads and that of the H4 mutant by dots. D = deproteinized genomic DNA treated in vitro with 1.25 units/mL MNase. M = molecular weight marker. The schematic vertical map on the left summarizes the nucleosomal organization of wild-type (gray semicircles) and *sir3* (empty semicircles). The map underneath the panel indicates the location of probe 1 and of the *Bam*HI site.

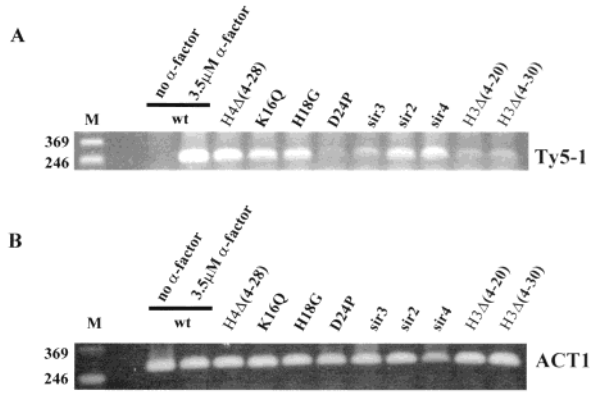

FIGURE 6: Transcriptional analysis of Ty5-1 in strains carrying mutations of histones H3 and H4 and of *SIR* genes. Panel A: RT-PCR analysis of Ty5-1 expression in all the strains used in this study, namely, H4Δ(4−28), K16Q (Lys16Glu, strain LJY912), H18G (His18Gly, strain LJY933), D24P (Asp24Pro, strain LJYD24P) *sir3*, *sir2*, *sir4*, H3Δ(4−20), and H3Δ(4−30), shows Ty5-1 expression, with differences in the intensity of the 230 bp band among strains. As a control for repression and expression of Ty5-1, the result of the RT-PCR assay of the wild-type and of the α-factor-treated wild-type, respectively, is reported. Panel B: Amplification of the ACT1 transcript from each RNA preparation, as an internal control. M = molecular weight marker. The oligonucleotides used for the PCR step of the assay are described in Materials and Methods.

is always lower than that caused by loss of the N-tail of H4 (*12*).

Our analyses of the Ty5-1 chromatin structure in strains lacking the terminal portion of histone H3 are in agreement with the behavior described for this histone. The MNase cleavage analysis of two strains carrying a 4−20 (lanes 4−6) and a 4−30 (lanes 7−9) amino acid deletion of H3, respectively, is shown in Figure 5. Their profiles were compared with that of the 4−28 deletion of histone H4 (lanes 10−12), which is marked by black dots (see also Figure 3). It is evident that both H3 mutants display in this region a MNase cleavage pattern different from that of the wild-type. This pattern, though, is not as well defined as the H4Δ(4−28) mutant. The LTR region in both mutants is in general strongly hyperaccessible to MNase, but a precise profile of alternate bands is only slightly evident. Moreover, the size of the bands indicated by black diamonds is rather different from that of the bands in the H4Δ(4−28) strain.

This experiment points out that, as in the case of the SIR proteins, different histones play different roles in the nucleosomal organization of repressive structures, since their mutation differently affects the chromatin profile.

Transcriptional Analysis of Heterochromatin Mutants. We show here that all of the mutant strains analyzed for chromatin structure undergo the loss of transcriptional silencing at telomeres that was previously reported in few instances (*2*, *12*, *13*, *29*, *30*). We analyzed the Ty5-1 transcripts in cells grown to the exponential phase (about 0.3−0.4 OD_{600}/mL), treated the transcripts with DNase I, and subjected them to RT-PCR analysis using the two oligonucleotides already described for the α-factor-treated cells (Figure 1). Expression of Ty5-1 in α-factor-treated cells was taken as reference for the correct band size.

The results reported in Figure 6, panel A, show that all of the mutants yield the diagnostic 230 bp band, indicating that Ty5-1 is transcribed in all strains, while in the wild-type untreated cells the amplification product is completely absent (see wild type, no α-factor). The intensity of the Ty5-1 band (panel A) differs from strain to strain, although there is no direct correlation between the amount of transcription and the extent of chromatin modification observed in the MNase profiling. In fact, while the RT-PCR product in α-factor-treated cells is intense, the MNase profile of these cells is not drastically changed (Figure 2A, lanes 5−8). Conversely, a mutant such as D24P shows a clearly alternative pattern of MNase digestion (Figure 4, lanes 9 and 10) while its Ty5-1 expression appears rather low. As an internal control from each sample, we amplified transcripts specific for the actin gene (*ACT1*, panel B). To ensure the quantitative meaningfulness of RT-PCR assays, each reaction was performed on the same amount of total RNA, under strictly controlled identical conditions. In addition, we also made sure to perform all experiments in the linear range of reactivity. Therefore, we can conclude that the reported analysis shows that all of the mutations cause disruption of the silencing heterochromatin structure and allow transcription.

Extent of Chromatin Modification in the Heterochromatin Mutants. Studies on silencing have revealed that the transcriptional repression caused by telomeric heterochromatin normally extends into the chromosome for up to 3−4 kb (*1*). Repression can spread further inside under specific

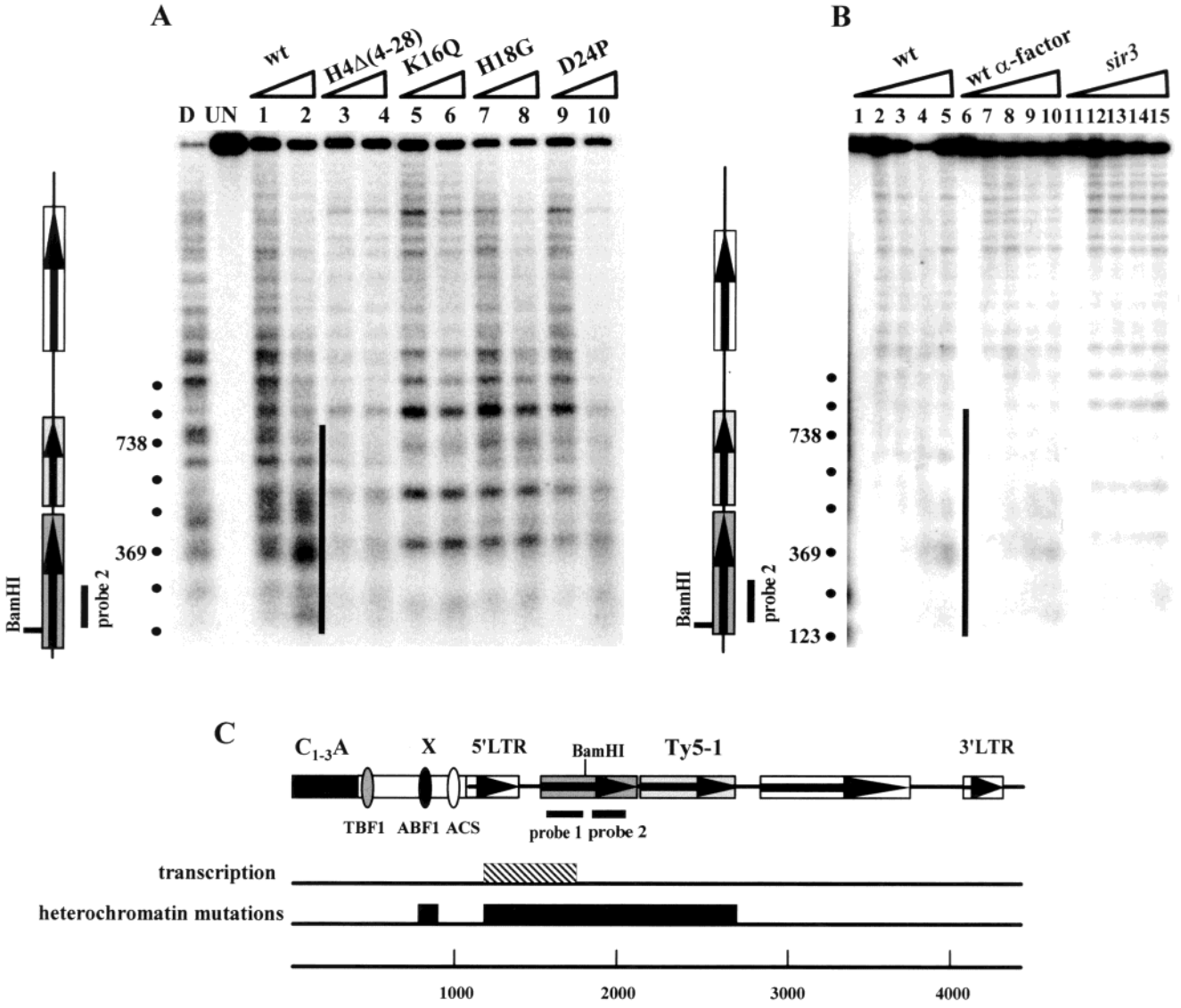

FIGURE 7: Extent of subtelomeric chromatin changes due to heterochromatin mutations and to α-factor-induced transcription. Panel A: To study the chromatin change due to heterochromatin mutations, the filter from the experiment shown in Figure 4 was stripped and rehybridized with probe 2, which allows mapping of MNase cleavage sites from the *Bam*HI site toward the more internal regions of the chromosome. The amounts of MNase used are described in Figure 4. All of the mutants show an identical profile, alternative to that of the wild type. The comparison of the MNase cleavage profile is between the wild-type strain (PKY501, lanes 1 and 2) and the H4 mutant strains, namely, H4Δ(4−28) (PKY813, lanes 3 and 4), K16Q (LJY912, lanes 5 and 6), H18G (LJY933, lanes 7 and 8), and D24P (LJYD24P, lanes 9 and 10). Panel B: Chromatin analysis of the α-factor-induced wild-type cells (lanes 6−10) in comparison with wild-type nontranscribing (lanes 1−5) and *sir3* (lanes 11−15) cells. The amounts of MNase used for each strain are 0, 1.25, 2.5, 5, and 10 units/mL. The extent of the region interested by the change in MNase cleavage distribution is indicated in both panels by a vertical bar. The position of probe 2 (described in Materials and Methods) is indicated in the vertical maps located on the left side of both panels. D = genomic DNA treated in vitro with 1.25 units/mL MNase. UN = untreated DNA. Panel C: Schematic representation of the region interested by chromatin modifications due either to transcription induced by α-factor (hatched box) or to mutations of heterochromatin components (black boxes).

conditions, i.e., in the case of overexpression of some components such as Sir3p (*31*).

We have extended the analysis of the Ty5-1 chromatin structure of all heterochromatin mutants to the more internal region to understand whether the nucleosomal rearrangement was a characteristic limited to the LTR of Ty5-1 or if a wider area is interested by this change. The filter used for the chromatin analysis of the H4 mutants shown in Figure 4 was stripped and rehybridized with probe 2 (pointing inward), which abuts the *Bam*HI site on the opposite side relative to probe 1 (pointing outward). The MNase cleavage profiles of these mutants are reported in Figure 7, panel A; the position of probe 2 is indicated in the map at the left side of the panel. The pattern of the wild-type strain is shown in lanes 1 and −2 of this panel. The accessibility to MNase of wild-type appears diffuse over an area encompassing the first and second open reading frames (the region is indicated by a vertical bar). A regular alternation of cleavage and protections is not evident in this area, suggesting that nucleosomes do not occupy precise translational positions. Our earlier studies described the presence of nucleosomes in this area, as shown by *nucleosomal spacing* analysis (*14*). Thus, nucleosomes are present but are not precisely positioned in the population. The MNase profile of wild type becomes regular, starting from a point coincident with the end of the vertical bar. This point maps at the end of the second ORF at about position 2650 from the extremity of the telomere.

Concerning the H4 mutants, they show MNase cleavage profiles rather different from that of the wild-type in the region defined by the vertical bar. In the mutants the profile is more regular, suggesting a rather homogeneous distribution of the nucleosomes. Starting from the region indicated by the end of the vertical bar, the mutants resume the wild-type profile. It is important that this point is located at about 2.65 kb from the end of the chromosome. In fact, telomeric silencing and heterochromatin have been described to normally extend inside the chromosome for about 3 kb. The MNase profiles obtained by analyzing the chromatins of the *sir3* (lanes 11−15, panel B) and *sir2* (not shown) are identical to those of H4, while the *sir4* profile strongly resembles that of wild-type (not shown). This implies that the integrity of the heterochromatin structure is required for the underlying nucleosomal distribution throughout the repressive area. Having found a different type of nucleosomal modification in the LTR of cells induced to transcribe by α-factor, as compared to those mutants in the heterochromatin components (see Figure 2A), we extended the chromatin analysis by comparing the results obtained with probe 2 on wild-type nontranscribing (lanes 1−5, panel B), *sir3* (lanes 11−15, panel B) and pheromone-treated wild-type (lanes 6−10, panel B) cells. The MNase profile of cells treated with the pheromone is the same as that of wild type nontranscribing cells, indicating that the nucleosomal modifications (namely, increased accessibility to MNase) observed upon induction is limited to the LTR area (Figure 2A) and is a specific characteristic of the regulatory region. This situation is schematically depicted in panel C. The drawing indicates the extent of chromatin modifications in the two conditions, i.e., transcription induced by α-factor (hatched box) and heterochromatin mutations (black boxes).

DISCUSSION

The dynamics of formation of telomeric heterochromatin, despite the large body of studies in the field, is still poorly understood. In addition, the relationship between the basic nucleosomal organization in chromatin and the higher order structures was not investigated in detail. We have determined how loss of silencing, brought about by different genetic and transcriptional conditions, can affect the subtelomeric chromatin structure in the left telomere of chromosome III of *S. cerevisiae*.

Chromatin Structure of Ty5-1 in Conditions of Transcriptional Induction by α-Factor. The starting point of this work is the study of the transcriptional induction of a Ty5-1 element located in subtelomeric position at LIII. Retrotransposons were shown to choose heterochromatin locations as sites of preferred transposition (*19*). Moreover, transcription of Ty5 elements introduced in heterochromatin was shown to be induced by the pheromone response pathway triggered by α-factor (*21*). Nonetheless, evidence for induction of the Ty5-1 element naturally present at LIII was not as yet available. Our earlier results demonstrated that Ty5-1 is not expressed in wild-type cells but can be activated by mutations of heterochromatin components, such as deletion of *SIR3* and of the N-terminus of histone H4 (*13*). We therefore asked whether in wild-type cells the Ty5-1 could be induced by other types of stimuli such as treatment with α-factor. The results of RT-PCR assays of RNA extracted from cells treated with the pheromone clearly show expression of Ty5-1 (Figure 1B), indicating that loss of heterochromatin components is not the only condition in which Ty5-1 can be transcribed. This implies that silenced chromatin in specific conditions can be accessed by the transcriptional machinery, as was also recently described (*23*). It was shown, in fact, that Pol II and TBP can be recruited to repressive heterochromatin following binding of the activator protein Hsf.

Few observations are available regarding the state of the subtelomeric chromatin in conditions of induced transcription. A recent work has described disruption of the core heterochromatin by eliminating telomere looping, following induction of transcription through the telomeric repeated sequences from a GAL_{UAS} promoter (*24*). Moreover, our previous work showed that the three nucleosomes in the LTR region of Ty5-1, which contains all of the regulatory sequences, adopt an alternate configuration in the *sir3* and H4Δ(4−28) mutant strains (*14*, *15*). The analysis of the nucleosomal organization of the Ty5-1 in cells induced to transcribe by α-factor provides further insight in the dynamics of subtelomeric chromatin. We found that the borders of the nucleosomes in the LTR become more accessible to MNase, likely indicating a less tight positioning. Nonetheless, the overall profile resembles that of the untreated nontranscribing cells, therefore being profoundly different from that of the *sir3* strain (the profiles are compared in panels A and B of Figure 2). The outcome is that transcriptional derepression is not sufficient to cause the alternate configuration of the nucleosomes but that this latter is linked to the presence/absence of heterochromatin components.

These results show that the integrity of the higher order heterochromatin structure is necessary for the specific positioning of the underlying nucleosomes, while in order to support the α-factor transcription a localized destabilization of nucleosomes in the LTR is sufficient.

Influence of Heterochromatin Mutations on the Nucleosomal Organization of the LIII Subtelomeric Region. We have extended the analysis of the chromatin structure of the LIII subtelomeric region to several strains bearing mutations either in the *SIR* genes or in the N-terminal tails of histones H3 and H4 to understand in more detail the relative importance of each heterochromatin component on the nucleosome organization of the subtelomeric region and of the Ty5-1 LTR. The comparison of the MNase profiles reveals differences in the cleavage pattern among strains.

For what concerns the *sir* strains (shown in Figure 3) it can be noted that the profiles of *sir3* and *sir2* are identical and differ from the wild type, while that of the *sir4* strain shows a composition of bands intermediate between the wild-type and the *sir3*-like patterns.

It is known that Sir3p and Sir4p directly interact with the histone tails, while Sir2p takes part in the complex only through interaction with Sir4p (*7*, *9*). Nevertheless, the influence of Sir2p on the nucleosome organization is more pronounced than that of Sir4p. This may reflect a hierarchy of importance of each element in the nucleosome positioning. A staple-like function was hypothesized for Sir3p by X-ray diffraction studies (*32*, *33*), directly involving Sir3p in the interaction between adjacent nucleosomes. This function has not been demonstrated as yet, and this hypothesis was unsupported until the recent work on *Drosophila*, showing the direct binding for another heterochromatin component, HP1, to the methylated N-terminal tail of histone H4. HP1

was proposed to act as a bridge between nucleosomes and non-histone proteins to form higher order chromatin structures. On the other hand, although not directly bound to histones, Sir2p may contribute to the establishment of the repressive structure through its recently described deacetylase activity (*10*, *11*), deacetylation of lysines being one of the hallmarks of the repressive heterochromatin. In this scenario it is conceivable that Sir4p only partially or indirectly contributes to the positioning of nucleosomes through its interaction with Sir3p, being its function of a possibly different nature.

The H4 mutants, conversely, show a more homogeneous behavior. We have chosen strains carrying amino acid substitutions in the domain which was reported to interact in vitro with Sir3p and Sir4p (*9*). In addition, these mutations cause loss of silencing (*29*) in vivo. All of the strains analyzed show a MNase cleavage profile identical to that of the H4Δ(4−28), whose nucleosomal configuration is the same as the *sir3* strain (*15*). This result points to the absolute relevance of the domain (aa 16−29; *29*) engaged in the binding with heterochromatin proteins, reinforcing the concept that the formation of a tight supramolecular complex can determine the positioning of the underlying nucleosomes.

Histone H3 was also shown to participate in the binding with the SIR proteins, therefore stabilizing the heterochromatin structure. Deletions of the N-terminal tails of H3 also affect silencing (*12*) although to a lesser extent than mutations of H4. In addition to being transcribed less than other mutants, the chromatin profiles of the N-terminal deletion mutants of H3 are clearly less defined than those of H4, showing a general increase in the MNase accessibility, devoid of a precise patterning of bands.

As in the case of the SIR proteins, also the contribution of the histones to the formation of heterochromatin may be differential and mediated through alternative mechanisms.

The transcriptional analysis of the strains used shows that all of the mutations tested allow transcription of Ty5-1 to different extents (Figure 6, panel A).

Heterochromatin Modifications: How Far Do They Extend? Silencing was shown to extend inside the chromosome for about 3−4 kb (*1*). From a structural point of view this characteristic was confirmed by chromatin immunoprecipitation analysis, which defined the region engaged in the interaction with the SIR proteins, allowing the authors to propose the looping model of the telomere (*7*, *8*).

We have investigated the extent of chromatin modifications by the MNase cleavage assay of all of the mutant strains used in this study, defining the pattern of cleavage in the internal region of the Ty5-1 (Figure 7, panel A). The accessibility to MNase in this region in wild-type cells appears quite diffuse and irregular. The presence of nucleosomes in this area was already established by the nucleosomal spacing analysis (*14*). Consequently, the absence of a regular pattern of cleavage and protection suggests that nucleosomes do not adopt precise translational positions.

Concerning the *SIR* and the H4 mutants (H4, Figure 7, panel A; *sir3*, Figure 7, panel B; *sir2* and *sir4*, not shown), it appears that, with the exception of *sir4* whose MNase profile resembles that of the wild type, all of them present an alternate chromatin configuration as compared to the wild type. The area interested by the alternate configurations (indicated by the vertical bar in Figure 7) extends to about 2.65 kb from the very end of the chromosome and is therefore in agreement with all of the reports showing for heterochromatin and silencing an extension of about 3 kb.

Remarkably, only the *sir4* strain shows modifications inside the X element. This indicates, as mentioned above, that different components may have different roles in subregions of telomeric heterochromatin. This observation may also be correlated to the discontinuity of silencing effects that were described for X and Y′ containing natural telomeres (*34*, *35*).

One interesting observation comes from the chromatin analysis of the internal region of Ty5-1 of the α-factor-treated, transcribing cells. The fact that the profile is identical to that of wild-type nontranscribing cells is particularly telling, since it indicates that transcription per se is not sufficient to induce extended nucleosomal alterations. The increased accessibility is limited to the LTR regulatory region, resembling more the situation of other euchromatic genes subjected to several types of chromatin remodeling. The alterations linked to the lack of heterochromatin components are of a more structural and global nature.

ACKNOWLEDGMENT

We thank M. Grunstein for the gift of all yeast strains used in this work.

REFERENCES

1. Gottschling D. E., Aparicio, O. M., Billington, B. L., and Zakian, V. A. (1990) *Cell 63*, 751−762.
2. Aparicio, O. M., Billington, B. L., and Gottschling, D. E. (1991) *Cell 66*, 1279−1287.
3. Moretti, P., Freeman, K., Coodly, L., and Shore, D. (1994) *Genes Dev. 8*, 2257−2269.
4. Wotton, D., and Shore, D. (1997) *Genes Dev. 11*, 748−760.
5. Tsukamoto, Y., Kato, J., and Ikeda, H. (1997) *Nature 388*, 900−903.
6. Martin, S. G., Laroche, T., Suka, N., Grunstein, M., and Gasser, S. M. (1999) *Cell 97*, 621−633.
7. Strahl-Bolsinger, S., Hecht, A., Luo, K., and Grunstein, M. (1997) *Genes Dev. 11*, 83−93.
8. Grunstein, M. (1998) *Cell 93*, 325−328.
9. Hecht, A., Laroche, T., Strahl-Bolsinger, S., Gasser, S. M., and Grunstein, M. (1995) *Cell 80*, 583−592.
10. Imai, S.-i., Armstrong, C. M., Kaeberlein, M., and Guarente, L. (2000) *Nature 403*, 795−800.
11. Landry, J., Slama, J. T., and Sternglanz, R. (2000) *Biochem. Biophys Res. Commun. 278*, 685−690.
12. Thompson, J. S., Ling, X., and Grunstein, M. (1994) *Nature 369*, 245−247.
13. Vega-Palas, M. A., Venditti, S., and Di Mauro, E. (1997) *Nat. Genet. 15*, 232−233.
14. Vega-Palas, M. A., Venditti, S., and Di Mauro, E. (1998) *J. Biol. Chem. 273*, 9388−9392.
15. Venditti, S., Vega-Palas, M. A., and Di Mauro, E. (1999) *J. Biol. Chem. 274*, 1928−1933.
16. Zhao, T., Heyduck, T., Allis, C. D., and Eissemberg, J. C. (2000) *J. Biol. Chem. 275*, 28332−28338.
17. Bannister, A. J., Zegerman, P., Partridge, J. F., Miska, E. A., Thomas, J. O., Allshire, R. C., and Kouzarides, T. (2001) *Nature 410*, 120−124.
18. Lachner, M., O'Carrol, D., Rea, S., Mechtler, K., and Jenuwein, T. (2001) *Nature 410*, 116−120.
19. Zou, S., Wright, D. A., and Voytas, D. F. (1995) *Proc. Natl. Acad. Sci. U.S.A. 92*, 920−924.
20. Zou, S., Ke, N., Kim, J. M., and Voytas, D. F. (1996) *Genes Dev. 10*, 634−645.
21. Ke, N., Irwin, P. A., and Voytas, D. F. (1997) *EMBO J. 16*, 6272−6280.

22. Aparicio, O. M., and Gottschling, D. E. (1994) *Genes Dev. 8*, 1133−1146.
23. Sekinger, E. A., and Gross, D. S. (2001) *Cell 105*, 403−414.
24. de Bruin, D., Kantrow, S. M., Liberatore, R. A., and Zakian, V. A. (2000) *Mol. Cell. Biol. 20*, 7991−8000.
25. Venditti, S., and Camilloni, G. (1994) *Mol. Gen. Genet. 242*, 100−104.
26. Wu., C. (1980) *Proc. Natl. Acad. Sci. U.S.A. 82*, 4374−4378.
27. Schmitt, M. E., Brown, T. A., and Trumpower, B. L. (1990) *Nucleic Acids Res. 18*, 3091−3092.
28. McCaffrey, G., Clay, F. J., Kelsay, K., and Sprague, G. F., Jr. (1987) *Mol. Cell. Biol. 7*, 2680−2690.
29. Johnson, L. M., Fisher-Adams, G., and Grunstein, M. (1992) *EMBO J. 11*, 2201−2209.
30. Vega-Palas, M. A., Martín-Figueroa, E., and Florencio, F. J. (2000) *Mol. Gen. Genet. 263*, 287−291.
31. Renauld, H., Aparicio, O. M., Zierath, P. D., Billington, B. L., Chhablani, S. K., and Gottschling, D. E. (1993) *Genes Dev. 7*, 1133−1145.
32. Luger, K., Mäder, A. W., Richmond, R. K., Sargent, D. F., and Richmond, T. J. (1997) *Nature 389*, 251−260.
33. Rhodes, D. (1997) *Nature 389*, 231−233.
34. Fourel, G., Revardel, E., Koering, C. E., and Gilson, E. (1999) *EMBO J. 18*, 2522−2537.
35. Pryde, F. E., and Louis, E. (1999) *EMBO J. 18*, 2538−2550.

BI016052Y